Vapor phase oxidation of dimethyl sulfide with ozone over V_2O_5/TiO_2 catalyst

Endalkachew Sahle-Demessie *, Venu Gopal Devulapelli

U.S. Environmental Protection Agency, Office of Research and Development, National Risk Management Research Laboratory, 26 W. Martin Luther King Drive (MS 443), Cincinnati, OH 45268, United States

ARTICLE INFO

ABSTRACT

The removal of volatile and odorous emissions from pulp and paper industrial processes usually generates secondary pollution which is treated further by scrubbing, adsorption, and catalytic incineration. Studies using a flow reactor packed with 10% vanadia/titania (V_2O_5/TiO_2) catalyst showed complete conversion of dimethyl sulfide (DMS) in the presence of ozone. The molar yields of partial oxidation products were only 10–20%. Small amounts of partial oxidation products, such as and dimethyl sulfone ($DMSO_2$), dimethyl disulfide (DMDS), and dimethyl sulfoxide (DMSO), were also formed. The results of the oxidation of DMS using ozone only, ozone plus catalyst, and oxygen plus catalyst suggest that the combined use of O_3 with catalyst is essential for the complete destruction of DMS to CO_2 and SO_2. A Box-Behnken design was used to determine the factors that have a significant effect on the conversion and selectivity of the products. It was concluded that product selectivity is strongly influenced by temperature, gas hourly space velocity (GHSV), and ozone concentration. The catalysts were characterized using XRD, surface area measurements, and SEM techniques. Time-on-stream studies carried out in a 500 ppmv gas stream held at 150 °C for 6 h, using 2 g of the catalyst, an ozone-to-DMS molar ratio of 0.9, and a GHSV of 37,000 h^{-1}, yielded 99.9% conversion of DMS. A plausible reaction mechanism has been proposed for the oxidation of DMS based on reaction product distribution and possible intermediates formed.

Published by Elsevier B.V.

1. Introduction

Odorous emissions from pulp and paper, wastewater treatment, and livestock production plants have been serious problem. The pulp and paper industry is one of the largest generators of pollutants, releasing high volumes with low concentration (HVLC) hazardous air pollutants, including more than 144 million tons of volatile organic compounds (VOCs) and 2×10^5 kg of toxic substances annually [1–4]. These vented gases contain reduced sulfur compounds that may present offensive odor at extremely low concentrations. Methanethiol (MT), hydrogen sulfide (H_2S), dimethyl sulfide (DMS), and dimethyl disulfide (DMDS) are emitted at concentrations as high as 19,000 ppm [5].

Currently, the pulp and paper industry collects non-condensable waste gas streams from the pulp mill through extensive ductwork from various sources and burns them in a thermal oxidizer [6]. Other methods used to abate VOCs include absorption using wet scrubbers, adsorption, and condensation. Removal of odorous methanethiol from the air or any other stream can also be

achieved by catalytic oxidation and chemisorption on impregnated activated carbon, activated by species such as NaOH, Na_2CO_3, and NH_3 [5–9]. However, the regeneration or disposal of substantial quantities of spent carbon is difficult. Moreover, the catalytic oxidation of methanethiol over cobalt molybdate catalysts can be employed to control the concentration to acceptable odor levels at a temperature of ∼400 °C [6], but the sulfur-containing VOCs that are produced have a poisoning effect on the catalyst, especially at lower temperatures (e.g., 300 °C) [7]. Unlike the oxidation of sulfur compounds in flames, which occurs at temperatures above 1600 K [10], catalytic oxidation and adsorption can be performed at lower temperatures (room temperature to ∼400 °C) but they are adapted only to low concentrations of methanethiol [11].

The oxidation of H_2S and ethanethiol using oxygen and fly ash resulted in up to 50% removal efficiency. However, similar results were not achieved for DMS and DMDS [12]. The catalytic oxidation of reduced sulfur compounds with oxygen over metal oxide catalysts, such as alumina-supported copper molybdenum oxide, showed high activity over a temperature range of 200–400 °C when applied to low inlet concentrations (100 ppm) [13–15]. However, the catalyst was poisoned significantly by sulfur. Other studies have shown Cr_2O_3/Al_2O_3 to be an efficient catalyst for the oxidation of DMS; both DMS and DMDS had the poisoning effect

* Corresponding author. Tel.: +1 513 569 7739; fax: +1 513 569 7677.
E-mail address: sahle-demessie.endalkachew@epa.gov (E. Sahle-Demessie).

on MnO/Fe_2O_3 catalysts [16]. The poisoning effect of sulfur on both the catalysts was not significant once the operating temperature exceeded 350 °C. Environmentally benign, cost-effective treatment technologies are needed to reduce the emission of VOCs and sulfur compounds emitted from pulp and paper industrial processes.

The use of ozone catalytic oxidation for the treatment of air polluted with VOCs has shown promise because higher conversions can be achieved at lower reaction temperatures when compared with those achieved with processes using catalytic oxidation and molecular oxygen [17–19]. Ozone is a clean oxidant which has a high thermodynamic oxidation potential, thereby offering the advantage of performing the reactions at low temperatures. The oxidation of oxalic acid was achieved with O_3 and dissolved cobalt (II) [19] or with O_3 and activated carbon where •OH were generated [20]. There has been limited research on the gas phase catalytic ozonation of air pollutants and odor-causing compounds such as sulfides, mercaptans, and aldehydes. The use of ozone as an oxidant for the oxidation of H_2S, methanethiol, DMS, and DMDS using wood fly ash as an inexpensive catalyst at a low temperature of 25 °C was reported [21,22]. The process oxidized 90–95% of an 85 ppmv DMS, stream and 50% of a 100 ppmv DMDS stream using 2 g of wood ash at a GHSV of 720 h^{-1} and an ozone concentration that ranged from 100 to 300 ppmv.

The objective of this study was to evaluate the combined use of ozone and a vanadia/titania (V_2O_5/TiO_2) catalyst for the oxidation of organic sulfur compounds in the gas phase. V_2O_5/TiO_2 catalysts have been found to be effective in the destruction of VOCs such as methanol [22–25]. Supported V_2O_5/TiO_2 catalysts exhibited resistance against SO_2 poisoning [26], which is important since there is a significant amount of total reduced sulfur emissions in HVLC emission streams from a Kraft mill [1,4]. Our goal was to assess the feasibility of ozone-enhanced catalytic oxidation of low concentration reduced sulfur compounds using DMS as a model molecule. This study intended to gain insight into the reaction pathway for the DMS oxidation, the effects of process variables on the catalyst activity, and the long-term effectiveness of catalytic ozone oxidation.

2. Experimental

2.1. Catalyst preparation

The oxidation of DMS with ozone was carried out over vanadia supported on titania catalysts. These catalysts were selected because they are currently used as complete catalytic oxidation catalysts for several total reduced sulfur compounds, and they have demonstrated resistance to fouling by sulfur, with or without further modification with promoters. The catalysts were prepared by impregnation and sol–gel methods.

The impregnation was achieved by soaking the support material (TiO_2, P25 Degussa) in a 50 ml aqueous solution of ammonium metavanadate and oxalic acid for 2 h and subsequent water evaporation in an oven. The metal-impregnated catalyst was obtained by drying the material in a vacuum oven at 110 °C for 6 h. The resulting powder was sieved through a 12 and an 8 mesh screens, giving particles between particle sizes of 1.6 and 2.3 mm, before it was calcined in air at 450 °C for 4 h.

The catalysts, which consisted of V_2O_5 co-precipitated with TiO_2, were prepared by sol–gel synthesis using 8.93 g of V_2O_5 (Aldrich, USA, >99%) dissolved in 300 ml of 10% H_2O_2. The samples were precipitated with 56.97 g of titanium (IV) *iso*-propoxide (diluted in propanol) and stirred continuously at room temperature. The gel obtained was washed with deionized water and vacuum dried for 6 h. Then, it was then calcined at 450 °C for 4 h in dry air.

2.2. Catalyst characterization

X-ray diffraction (XRD) analyses were performed to characterize the bulk properties of the catalyst. The powder diffraction patterns were recorded on a Siemens D5000 diffractometer using a Cu Kα radiation source. The scans were performed over the 2θ range, from 20° to 60°, using a resolution of 0.017° and count time of 2 s at each point. The XRD was equipped with voltage and current stabilizers and a computer with software to record the diffraction patterns. The surface area of the catalyst, fresh and used, was measured using nitrogen adsorption at 77 K, and the Brunauer, Emmett and Teller (BET) method using a Micromeritics (AutoChem 2920) surface area analyzer. Prior to analyses, 0.2 g of the catalyst samples were loaded into a quartz reactor and degassed at 120 °C with a helium purge for 60 min. A five-point nitrogen (air product > 99.9%) adsorption isotherm was used to determine the BET surface area of the samples.

Scanning electron microscopy (SEM) and energy dispersive spectroscopy (EDS) X-ray microanalysis were performed to measure the mass and atomic ratios of vanadium and titanium in the catalyst samples.

2.3. Generation and quantification of ozone

A custom built annular gas phase corona reactor was used (Ceramatec Inc., Salt Lake City, UT) to generate ozone. The flow of dry oxygen gas was controlled through the reactor which can produce from 3 to 25 g/h of ozone. The corona reactor had to be cooled using a water jacket, and the maximum temperature in the ozone generator was less than 50 °C. The ozone dose to the reactor and residual amounts were measured using an iodometric titration method. The results were confirmed with an UV absorption technique using an Ozone Analyzer (Model-OLA, Ozone Services, Yanco Industries Ltd.) [27]. The resulting concentration of ozone decreased slightly as the flow rate of oxygen increased; however, the total amount of ozone increased as O_2 increased.

2.4. Catalytic activity measurements

Catalytic activity measurements were carried out in a continuous flow, fixed-bed reactor at atmospheric pressure. A detailed description and schematic representation of the experimental set-up are shown in Fig. 1. It consisted of a packed bed reactor (volume = 22 ml, height = 30.5 cm, i.d. = 0.476 cm) packed with 2 g of catalyst pellets (2 mm size) diluted with 4 g of glass beads (height of catalyst bed = 6 cm, volume of catalyst bed = 4.5 ml) in the middle of the reactor. The reactor was mounted vertically in an electrically heated split-furnace (Supelco). It was fed with a heated mixture of 1% (v/v) substrate (DMS) in ultra pure nitrogen that was mixed with ozone, oxygen, and a diluent stream of nitrogen. The residence time of the reactor was varied between 0.1 and 0.5 s, and the corresponding GHSV was varied from 18,785 to 75,000 h^{-1}. The inlet gas stream was supplied from a pressurized gas cylinder with premixed concentrations of 1% DMS in nitrogen (Wright Brothers Inc.). The flow rates of oxygen through the corona discharge ozone generator, nitrogen, and DMS in N_2 were adjusted using mass flow controllers (Sierra Instruments Inc.). Prior to the activity studies, the catalyst was activated at 150 °C in oxygen (50 cm^3/min) for 30 min. The by-pass line and effluent stream temperatures also were kept at 100 °C, allowing for the analysis of the gas stream prior to the reactor while minimizing the condensation of water and organics formed in the reactor.

The experiments were also divided into three parts. The first part was performed to compare the presence of ozone with that of
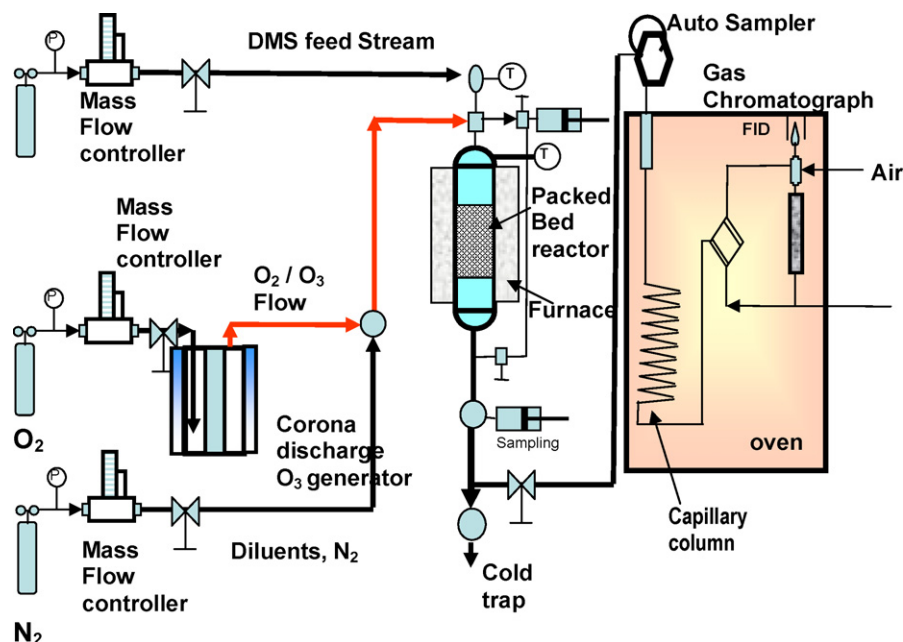
Fig. 1. Schematic diagram of test system for ozone-enhanced catalytic oxidation of dimethyl sulfide with ozone.

oxygen on the performance of catalytic conversion of DMS. The second part was a factorial design of the experiment to determine the effect of varying operating parameters. The parameters and ranges tested were inlet temperature (100–250 °C), O_3-to-DMS concentration ratio (0.45–1.8), and GHSV (18,785–75,000 h^{-1}). The third part was a test to determine the deactivation of the catalyst due to the potential sulfur poisoning effect in the oxidation of DMS at different reaction conditions. Purged N_2 carried the vaporized VOC to mix with dilution air and N_2 in the mixture to simulate the waste gas from a typical pulp digester blow tank.

2.5. Analytical procedure for catalytic oxidation of DMS with ozone

The catalytic oxidation of DMS with ozone involves the production of CO_2 and SO_2 as end products (i.e. complete oxidation products of DMS). The catalytic activity results were expressed in term of DMS conversion, and the calculations were based on the disappearance from the reactant flow. The outlet and inlet concentrations of DMS were determined using an in-line GC–FID:

$$DMS\ conversion = \frac{C_{DMS\ inlet} - C_{DMS\ outlet}}{C_{DMS\ inlet}} \times 100$$

The yield of each partial oxidation product is a ratio of molar concentration of the partial oxidation product formed and initial concentration of DMS. The concentrations of major partial oxidation products of DMS (DMDS, dimethyl sulfoxide (DMSO) and dimethyl sulfone (DMSO$_2$)) were determined by analyzing the concentrations at the reaction outlet using in-line GC–FID analysis. The selectivity of each partial oxidation product was calculated from the molar yield of the partial oxidation product and molar conversion of DMS.

$$selectivity\ of\ partial\ oxidation\ product$$
$$= \frac{molar\ yield\ of\ partial\ oxidation\ product}{molar\ conversion}$$

The combined selectivity of CO_2 and SO_2 was assumed as 100 minus the selectivity for the partial oxidation products.

2.5.1. Analysis of the gas phase

The concentrations of the organic compounds were measured with an Agilent 6890 Series GC that was equipped with a split/splitless injection (250 °C) and FID detector. The column used was a Supelco-Q^{TM}-plot (30 m × 0.32 mm # 33577-04A) capillary column. The samples were collected from the flowing influent and effluent streams, and they were introduced into the GC injection port with an in-line autosampling valve. The quantification of the results was achieved by performing the dynamic calibration of DMS and liquid calibrations of partial oxidation products (i.e. DMDS, DMSO and DMSO$_2$). For CO$_x$ analysis, an earlier established GC/FID method was followed [28].

2.6. Confirmation of the reaction products by GC–MS

The reactant DMS and major partial oxidation products (DMDS, DMSO and DMSO$_2$) were identified by comparing their GC retention times to those of pure compounds and also by analyzing them with a GC–MS (Thermo-Finnegan) using a Supelco-Q^{TM}-plot (30 m × 0.32 mm # 33577-04A) capillary column. The gas samples were collected from the reaction vent using a gas tight GC syringe and injected immediately into the GC–MS (Thermo-Finnegan) injection port. The GC–MS chromatogram and mass patterns for each compound are depicted in Fig. 2.

3. Results and discussion

3.1. Catalyst characterization

The XRD patterns of the V_2O_5/TiO_2 catalysts used during this study are shown in Fig. 3. The XRD patterns of the sol–gel catalyst show very weak diffraction signals of anatase (d values: $2\theta = 25.3$, 48.06, 53.9 ASTM# 86-1157), corresponding to the diffraction plane (1 0 1) of the anatase TiO_2 phase in all the calcined and used catalysts. No separate phase was observed in the XRD patterns for V_2O_5 species. However, the possibility cannot be ruled out for the presence of V_2O_5 crystallites less than 5 nm, because they are beyond the XRD detection limits.
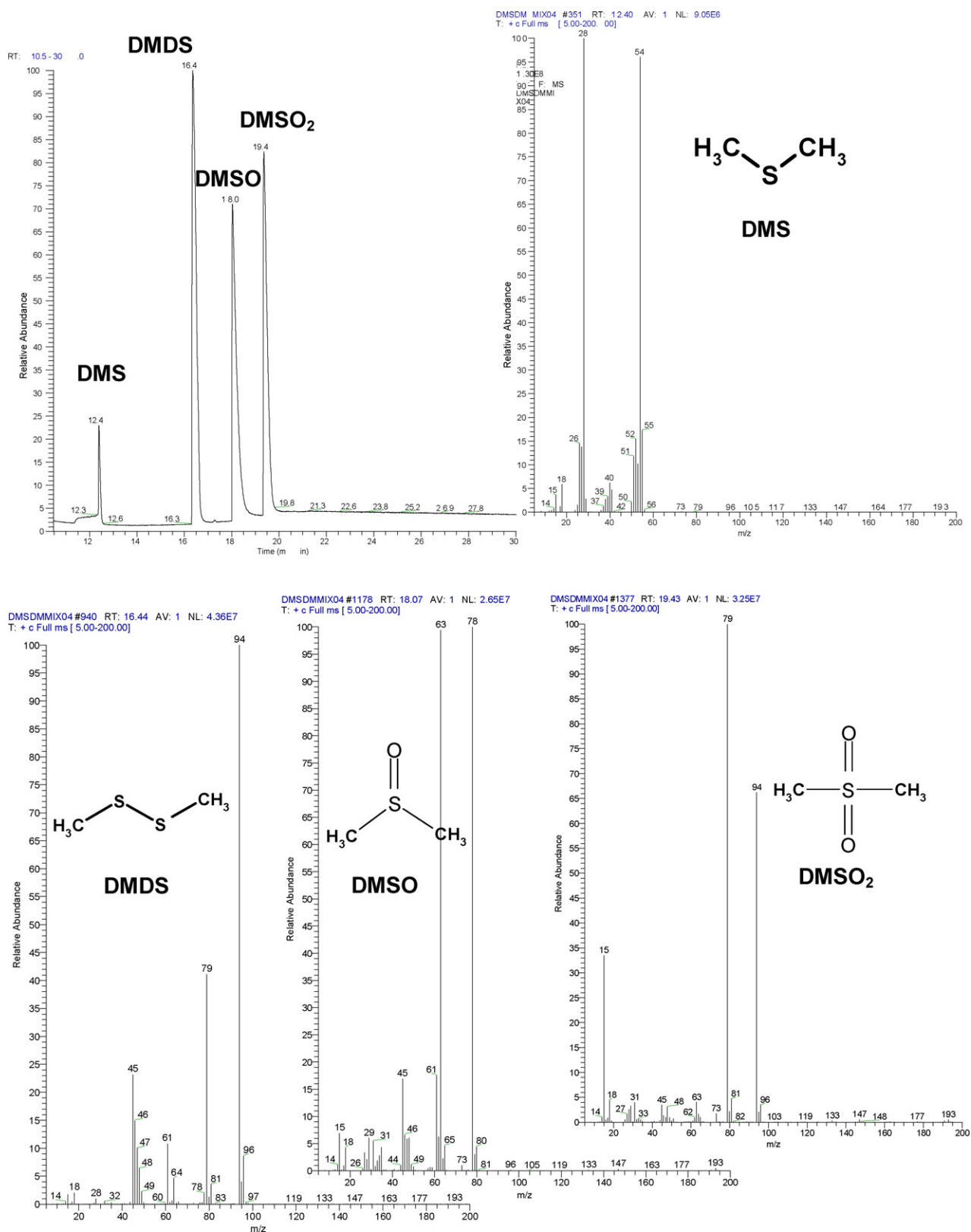
Fig. 2. Gas chromatographic-mass spectra of analysis of outlet stream sample from DMS oxidation with O_3 over 10% V_2O_5/TiO_2 catalyst at 100 °C, O_3-to-DMS mole ratio: 0.6, and GHSV: 37,000 h^{-1}.

The BET surface areas of the impregnated catalysts and the catalysts that were prepared by sol–gel are listed in Table 1. The catalysts that were prepared by sol–gel had a higher surface area as compared to the impregnated catalysts.

For both catalysts, the surface areas decreased after the reaction time of 6 h.

The SEM imaging analysis (Fig. 4) showed the narrow distribution of small particle size for sol–gel V_2O_5/TiO_2 catalyst
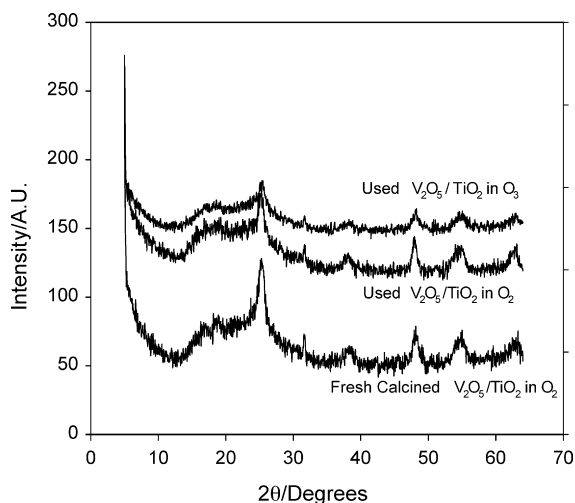
Fig. 3. X-ray diffraction patterns of sol–gel prepared V_2O_5/TiO_2 catalysts.

which is the reason for its high surface area compared to impregnated V_2O_5/TiO_2 catalyst.

3.2. Oxidation of DMS with ozone

Although, ozone is a strong oxidant, catalytic oxidation with ozone offers new low-temperature reaction a way to achieve higher rates and lower activation energies than catalytic oxidation with molecular oxygen. Prior to conducting the detailed catalytic oxidations studies, an exploratory investigation was conducted to evaluate the effect of ozone on the gas phase oxidation of DMS and catalytic oxidation with oxygen using a 10 wt.% V_2O_5/TiO_2-impregnated catalyst. Fig. 5 illustrates the results of the oxidation of DMS under the following oxidation conditions: ozone only

Table 1
BET surface area of fresh and spent (6 h run) V_2O_5/TiO_2 catalyst prepared by impregnated and sol–gel methods

Catalyst	BET surface area ($m^2 g^{-1}$)	
	Fresh	Spent
10 wt.% V_2O_5/TiO_2 (impregnated)	30.14	20.07
V_2O_5/TiO_2 (sol–gel)	142.7	107.5

(gas phase), ozone and catalyst, and oxygen and catalyst. The oxidation of DMS with ozone was carried out in the absence of a catalyst. The temperature range was 100–250 °C at an O_3-to-DMS ratio of 1.8. The complete conversion (99%) of DMS was achieved at all temperature ranges studied. However, the selectivity of the partial oxidation products decreased as the temperature increased. These results reveal that the increase in reaction temperature favors the conversion of partial oxidation products over deep oxidation products (i.e. carbon dioxide and sulfur dioxide). The results also indicate that more than the stoichiometric amounts of ozone are required for the deep oxidation of DMS to CO_2 and SO_2. The combined yield of complete oxidation products such as CO_x and SO_2 was determined based on moles of DMS converted minus yield of the partial oxidation products.

In order to understand the role of the oxidant, experiments to evaluate the oxidation of DMS with molecular oxygen over a 10% V_2O_5/TiO_2 catalyst were conducted. The results are depicted in Fig. 5. The conversion of DMS, as compared to the oxidation with ozone, was very low; the conversion increased slightly as the reaction temperature increased. It was also shown that the DMS oxidation results under various oxidation conditions, such as gas phase ozonation in absence of catalyst, catalytic oxidation with oxygen, and catalytic ozonation, were varied. It can be implied from the results shown in Fig. 5 that the use of ozone as oxidant is essential for the high conversions of DMS at low reaction
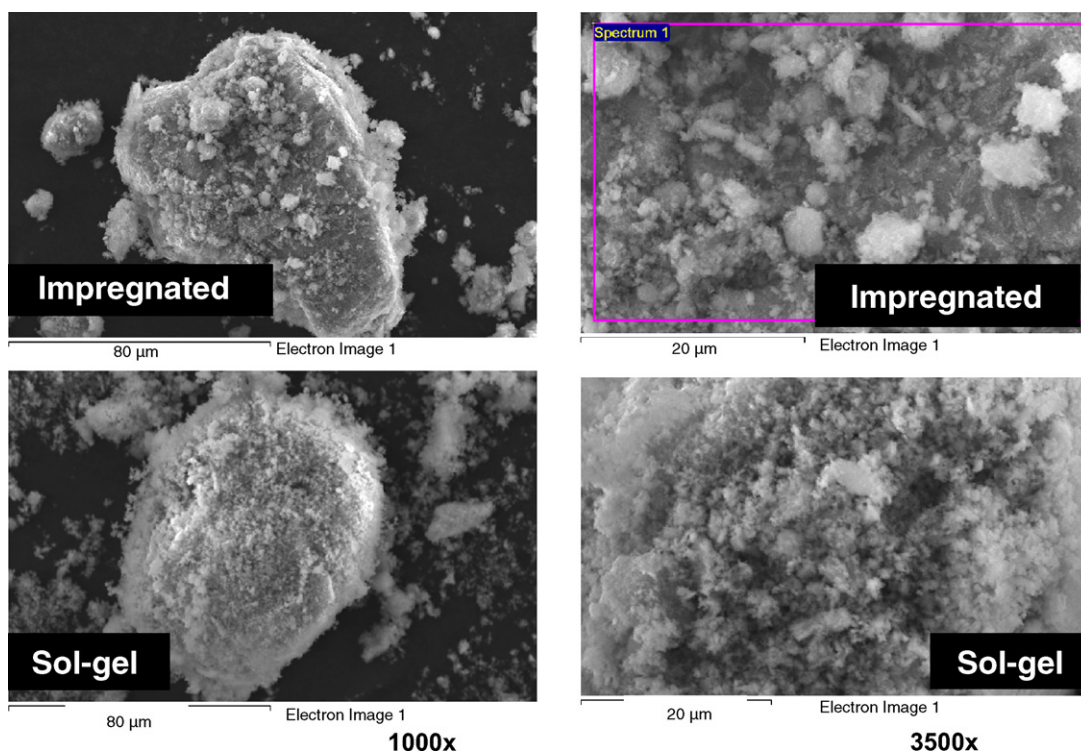

Fig. 4. Scanning electron micrograph analysis of impregnated and sol–gel prepared V_2O_5/TiO_2 catalysts.
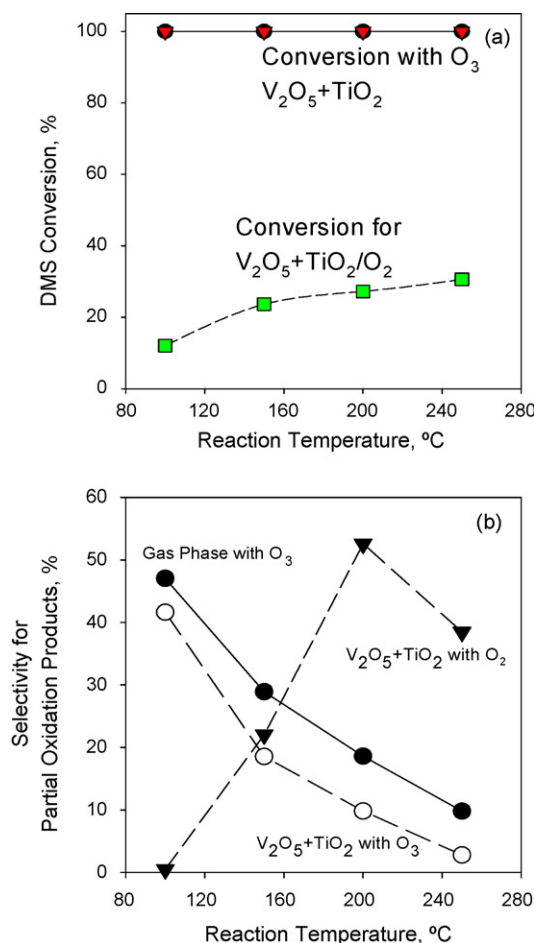
Fig. 5. Effect of temperature on oxidation of DMS with different oxidants: (i) without catalyst and ozone (gas phase), (ii) with catalyst and ozone and (iii) with catalyst and oxygen (a) DMS conversion; (b) selectivity of partial oxidation products.

Fig. 6. Conversion and selectivity for partial oxidation products for the oxidation of DMS with O_3 over 10% V_2O_5/TiO_2 (impregnated) and V_2O_5/TiO_2 (sol–gel, V/Ti: 0.5) catalysts. Inlet DMS concentration: 500 ppm; total flow rate: 1000 ml/min; temperature: 200 °C; catalyst weight: 2 g, O_3-to-DMS mole ratio: 1.8, GHSV: 37,000 h^{-1}.

temperatures. The data indicate the feasibility of complete degradation of DMS using catalytic ozonation at temperatures below 200 °C. The selectivity of partial oxidation products decreased which means the deep oxidation potential increased in order; catalytic oxidation with O_2 < gas phase oxidation with ozone < catalytic oxidation with ozone. This indicates that the combined use of ozone and the catalyst enhanced the deep oxidation of DMS. Other gas phase oxidation studies of DMS and O_3 at room temperature did not result in any measurable removal of DMS, indicating that a moderate temperature is needed to initiate the decomposition of ozone [22].

The oxidation of DMS with ozone was carried out over 10% V_2O_5/TiO_2 (impregnated) and V_2O_5/TiO_2 (sol–gel, V/Ti = 0.5) catalysts. From the results depicted in Fig. 6, under the current test conditions it can be seen that the method of catalyst preparation had minimal effect on the DMS conversion or the selectivity of partial oxidation products. The results also indicated that the high vanadium content and high surface area of the sol–gel catalyst did not affect the catalytic ozonation mechanism during the oxidation of DMS. In order to further study the effect of various reaction parameters, 10% V_2O_5/TiO_2 (impregnated) was chosen as the optimal catalyst.

3.3. Statistical design of the experiment

A Box-Behnken design was used to study the main effects and the quadratic and two-way interactions effects as a preliminary
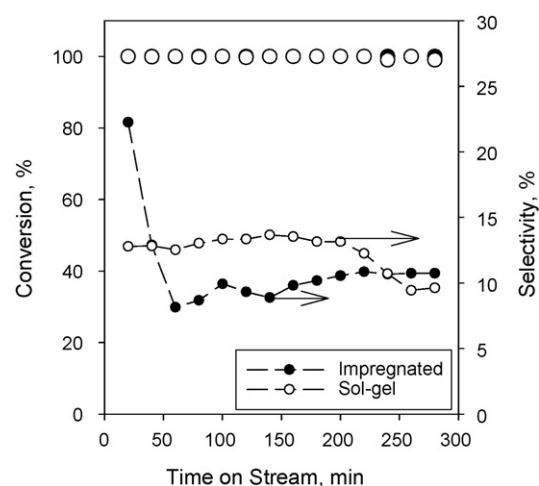
screen to identify the important factors. The design variables, described in coded and actual values, are listed in Table 2. The boundary conditions were as follows: x_1, temperature = 100–250 °C; x_2, ozone-to-DMS ratio = 0.4–1.8; x_3, GHSV = 18,785–75,000 h^{-1}. GHSV is defined as the volume of gaseous feed (measured at room temperature and 1 atm pressure) passed through a unit volume of the reactor per hour. Randomized "Box-Behnken design" [29] was then used to study the main effects of temperature, ozone concentration, and GHSV, and their interaction on the DMS conversion and selectivity for partial oxidation products. Within the design, a face-centered cubic design was used. The Box-Behnken design is an independent quadratic design because it does not contain an embedded factorial or fractional factorial design. The treatment combinations are at the midpoints of the edges of the process space and at the center. Regression equations were developed to correlate the relative importance of the effects of process variables on the conversion and product selectivity of DMS oxidation with ozone and V_2O_5/TiO_2 catalyst.

The dependence of DMS conversion and selectivity on temperature, ozone concentration, and GHSV for complete oxidation products may be estimated using a response function which is

Table 2
Box-Behnken factorial design with coded and actual independent variables

Run	Coded factors			Temperature (°C)	[O_3]/[TRS]	GHSV (h^{-1})
	x_1	x_2	x_3			
1	0	0	0	150	0.9	37,000
2	1	1	0	250	1.8	37,000
3	−1	−1	0	100	0.45	37,000
4	1	0	−1	250	0.9	18,785
5	0	0	0	150	0.9	37,000
6	0	1	1	150	1.8	75,000
7	1	−1	0	250	0.45	37,000
8	0	0	0	150	0.9	37,000
9	−1	0	1	100	0.9	75,000
10	−1	1	0	100	1.8	37,000
11	1	0	1	250	0.9	75,000
12	0	−1	−1	150	0.45	18,785
13	−1	0	−1	100	0.9	18,785
14	0	1	−1	150	1.8	18,785
15	0	−1	1	150	0.45	75,000

Table 3
Factors and levels for Box-Behnken design

Run	Temperature (°C)	O_3/DMS	GHSV (h^{-1})	Activity after 2 h run time		
				Conversion (%)	Selectivity of POP (%)	Selectivity of $CO_2 + SO_2$ (%)
1	150	0.9	37,000	99.9	38.0	62.0
2	250	1.8	37,000	99.9	2.8	97.2
3	100	0.45	37,000	76.2	17.3	82.7
4	250	0.9	18,785	99.9	5.3	94.7
5	150	0.9	37,000	99.9	29.2	70.8
6	150	1.8	75,000	99.4	46.0	54.0
7	250	0.45	37,000	99.0	12.7	87.3
8	150	0.9	37,000	99.9	38.0	62.0
9	100	0.9	75,000	99.9	21.7	78.3
10	100	1.8	37,000	99.9	37.1	62.9
11	250	0.9	75,000	99.9	27.6	72.4
12	150	0.45	18,785	99.9	7.5	92.5
13	100	0.9	18,785	99.9	6.9	93.1
14	150	1.8	18,785	99.9	2.9	97.1
15	150	0.45	75,000	97.8	26.0	74.0

based on the following general leaner regression equation:

$$Y_{ijk} = \beta_0 + \beta_1 X_1 + \beta_2 X_2 + \beta_3 X_3 + \beta_4 X_1 X_2 + \beta_5 X_1 X_3 + \beta_6 X_2 X_3 + \beta_7 X_1^2 + \beta_8 X_2^2 + \beta_9 X_3^2 + \varepsilon_{ijk} \quad (1)$$

where Y_{ijkm} is the response at the ith temperature level, jth ozone concentration, kth GHSV level, and mth replication, and ε_{ijkm} is the error which is assumed to be distributed normally with a mean of zero and variance of σ^2.

3.4. Effects of process variables

The results of DMS conversion and product selectivity after 2 h of run time are presented in Table 3. These runs were repeated twice.

The regression analyses were conducted to evaluate the value of the coefficients of the response function given in Eq. (1) and the effects of process factors on the conversion of DMS and product selectivity. The output shows the results of fitting a multiple linear regression model to describe the relationship between the DMS conversion and the three independent variables. The p values in the analysis of variance (ANOVA) were greater than 0.1 (table not shown) indicating that there is not a statistically significant relationship between the variables at the 90% or higher confidence intervals. The low R^2 statistics for the model fitting to the data confirmed this observation.

For product selectivity, the values of the coefficients for the ANOVA were generated using statistical analysis software, STATGRAPHICS Centurion (Hedron, VA, Version 5). The coefficients are listed in Table 4. The output shows the results of fitting a multiple linear regression model to describe the relationship between the total yield of complete oxidation product (Y) and the independent variables. The equation of the fitted model is

$$Y = 208.02 - 0.775X_1 - 57.33X_2 - 0.0018X_3 - 0.162X_1X_2 - 0.00033X_2X_3 + 0.0019X_1^2 + 17.81X_2^2 - 1.886 \times 10^{-8}X_3^2 \quad (2)$$

All except three of the p values in the ANOVA table are less than 0.05, indicating a statistically significant relationship between the variables at the 95% confidence level. The R^2 statistic indicates that the model, as fitted, accounts for 91.3% of the variability in the selectivity of the partial oxidation products. The model was simplified by removing the interaction effect X_1X_3 because the p-value was greater than 0.1 and the term is not statistically significant. The adjusted R^2 statistics, which are more suitable for

comparing models with different number of independent variables, is 83%. The standard error of the estimate is 6.35 with 6 degrees of freedom. This value can be used to construct the prediction limits for new observations.

The selectivity for complete oxidation products is shown in Fig. 7(a) and (b) as contour plots of Eq. (2) for a constant GHSV of 18,785 and 75,000 h^{-1}, respectively. This function displays curvature in its dependence for both temperature and ozone concentration, which is explained by the polynomial terms in Eq. (2). The catalyst system has been shown to be very promising since it gives 99% conversions at moderate-to-high GHSV and low temperatures to avoid waste gas reheating. It also shows that at a low GHSV and with increased contact times, there is more than an 80% chance of achieving complete oxidation products for all temperature ranges and ozone concentrations. For example, at a GHSV value of 18,785 h^{-1}, the selectivity for complete (99%) oxidation products increased fairly at a O_3-to-DMS ratio of 1 when the reaction temperatures were increased from 100 to 250 °C. However, the increase in ozone concentrations at a constant temperature and GHSV may result in more complex results because of competing surface and gas phase reactions which result in different product distributions.

Fig. 7(a) and (b) and Eq. (2) provide information useful for designing processes for catalytic removal of DMS. For example, the

Table 4
Regression analysis for selectivity of partial oxidation product

Independent variable	Parameter estimate	Standard error	t-Statistic	p-Value(t)
Slope	208.42947	29.62942	7.03454	0.0004
X_1	−0.77815	0.26068	−2.98507	0.0244
X_2	−57.43790	23.86667	−2.40662	0.0528
X_3	−0.00188	0.00053	−3.56839	0.0118
X_1^2	0.00192	0.00070	2.75004	0.0333
X_2^2	17.87037	8.61020	2.07549	0.0832
X_3^2	1.89E−8	5.06E−9	3.73595	0.0097
X_1X_2	0.16160	0.06132	2.63552	0.0388
X_2X_3	−0.00033	0.00016	−2.00430	0.0919

Source	Sum of squares	d.f.	Mean square	F ratio	p-Value
Analysis of variance					
Model	2710.02	8	3338.75	7.93	0.01055
Residual	256.39	6	42.73		
Total (correlation)	2966.41	14			

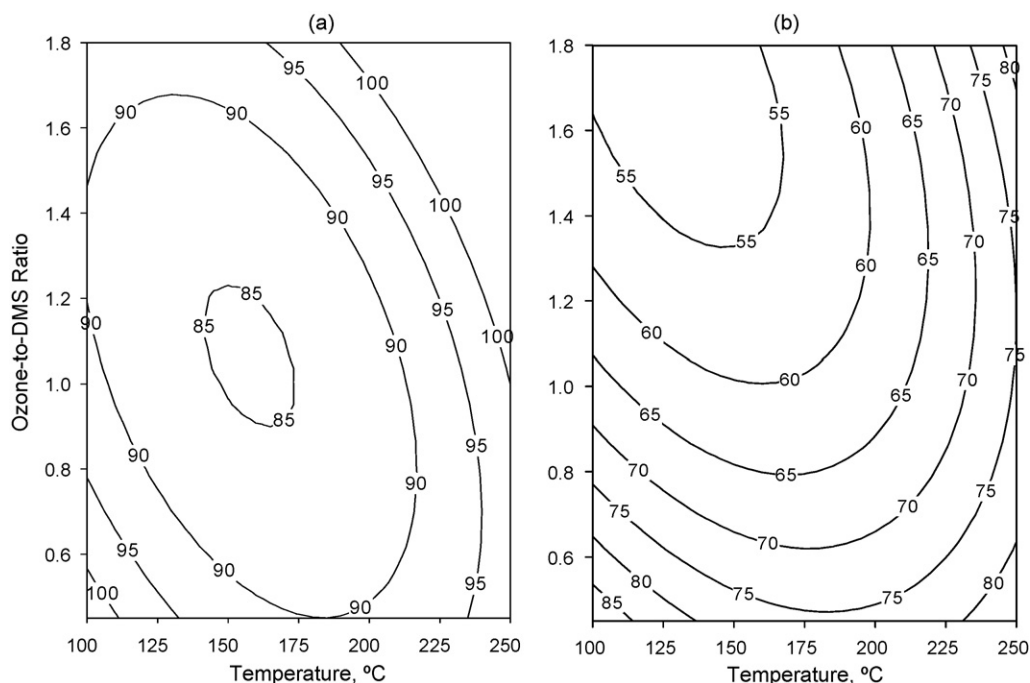X_1: temperature; X_2: O_3/DMS mole ratio; X_3: GHSV.

Fig. 7. Contour plots of selectivity for complete oxidation products of DMS versus temperature and ozone concentration for (a) GHSV of 18,785 h^{-1} and (b) GHSV of 75,000 h^{-1}.

presence of ozone is critical to the conversion of DMS, whereas selectivity for partial or complete oxidation of products may be improved through optimizing reaction temperatures and GHSV.

3.5. Effects of process variables on product distributions

The effects of temperature on product selectivity in the oxidation of DMS in the absence of and in the presence of ozone at an O_3-to-DMS molar ratio of 1.8 are shown in Fig. 8. The results suggest that the quantity and distribution of partial oxidation products are strongly affected by an increase in temperature and presence of O_2. As the reaction temperature was increased from 100 to 200 °C, both the total partial oxidation products and the major component of the partial oxidation products (DMSO$_2$) decreased.

In the absence of ozone in the inlet stream, the predominant product was DMSO (48%), and it increased as the temperature increased, up to 200 °C. Higher temperatures resulted in a decrease of DMSO and the generation of deeper oxidation products. In the presence of ozone, the major partial oxidation product was DMSO$_2$ (25%), with DMSO and DMDS being 14%, and 4%, respectively. As the temperature increased to 150 °C, the DMSO fraction was reduced to less than 4% and the primary partial oxidation product was DMSO$_2$. This implies high temperatures favor the complete oxidation of DMS to complete oxidation products such as CO$_2$ and SO$_2$. Unlike the oxidation with ozone, the use of oxygen as the oxidant produced DMSO as the major oxidation product and the DMSO$_2$/DMSO ratio increased as the reaction temperature increased. This implies that DMS oxidation with oxygen stops at the DMSO stage and very high temperatures are required for deeper oxidation of DMS.

The effects of the ozone concentration on product selectivity were studied by varying the O_3-to-DMS mole ratios from 0 to 1.8, at a reaction temperature of 200 °C and a GHSV of 18,785 h^{-1} (Fig. 9). The results show DMS conversions increased from 20% when the oxidant was only O_2 to 100% in the presence of O_3 and concentrations close to stoichiometric amounts for feed concentrations of DMS. These results are similar to the results reported by
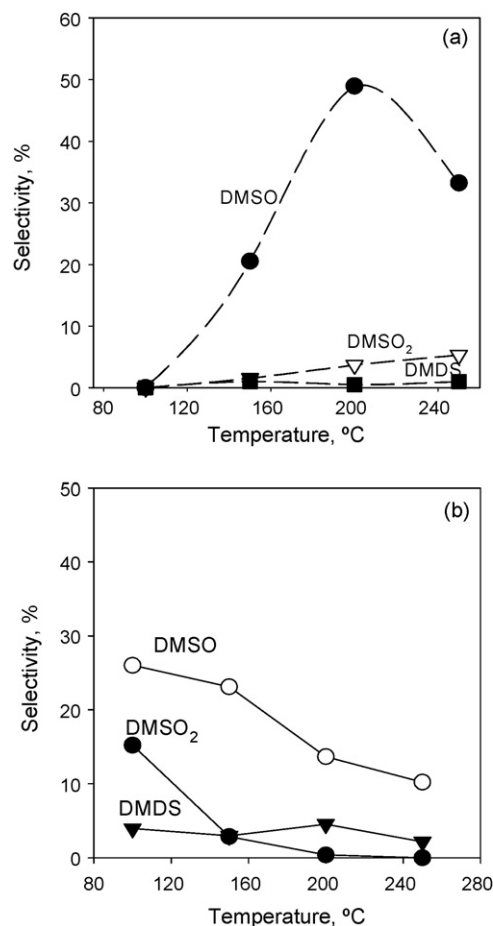

Fig. 8. Effect of temperature on the selectivity of partial oxidation products of DMS oxidation with O_3 or O_2 in presence of 10 wt.% V$_2$O$_5$/TiO$_2$ catalyst. Inlet DMS concentration: 500 ppm; total flow rate: 1000 ml/min; catalyst weight: 2 g, O_3-to-DMS mole ratio: 1.8 for (a) O_2 and (b) O_3.
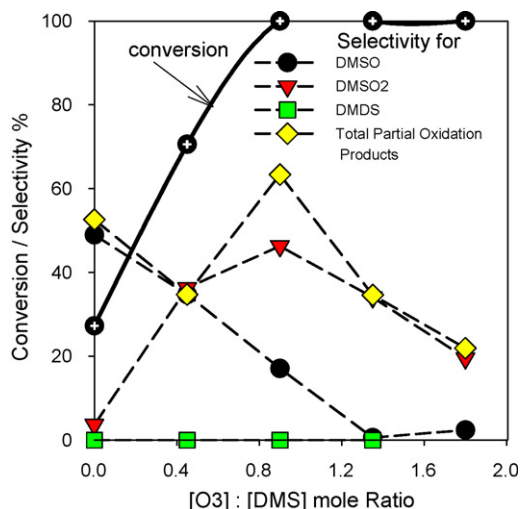
Fig. 9. Effect of ozone concentration on selectivity of partial oxidation products of gas phase oxidation of DMS with ozone. Inlet DMS concentration: 500 ppm; total flow rate: 1000 ml/min; reaction temperature: 200 °C.

Ross and Sood [6] and Chu and Horng [7] which showed that the adsorption and activation of the O_2 molecule on the catalyst surface requires higher temperatures is important in the process of catalytic incineration of methanethiol and DMS as described by the Langmuir–Hinshelwood model. However, the selectivity of the partial oxidation products decreased significantly with the increase in O_3-to-DMS mole ratios, from approximately 60% at a ratio of 0.45 to almost zero at a ratio of 1.8. This means that a high concentration of ozone enhanced both gas and surface oxidations to afford complete oxidation (99.9%) of DMS to CO_2 and SO_2 (total of 86%) at temperatures less than 250 °C. Other studies on the catalytic oxidation of DMS with O_2 suggest that the DMS intermediates of the reaction are the major components of the oxidized gas at lower temperatures. Essentially, the complete oxidation of DMS to CO_2 was not reached until the operating temperature was more than 380 °C [8].

3.6. Catalyst stability and time-on-stream studies

The effects of process conditions on the performance of a flow reactor packed with 10% V_2O_5/TiO_2 catalyst (selectivity and
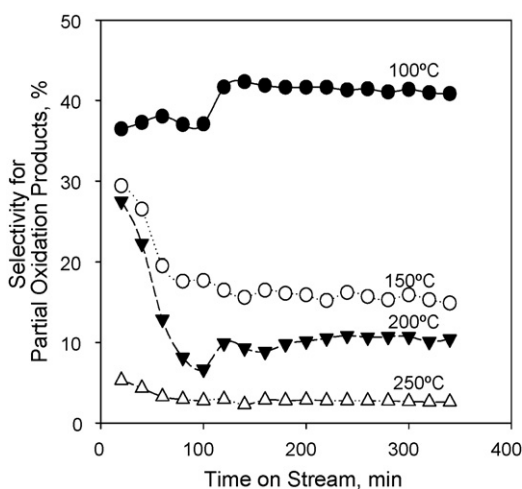

Fig. 11. Stability of 10 wt.% V_2O_5/TiO_2 catalyst for product selectivity of the oxidation of DMS with O_3 at selected ozone-to-DMS ratios. Inlet DMS concentration: 500 ppm; total flow rate: 1000 ml/min; temperature: 200 °C, catalyst weight: 2 g, GHSV: 18,785 h^{-1}.

stability with time) during DMS oxidation were studied. Catalyst activity for the complete conversion of DMS did not change with run time. Rather, catalyst activity increased slightly with the longer time-on-stream and increased reaction temperatures (Fig. 10). The product studies performed using the flow reactor with increased ozone concentrations at a constant temperature of 200 °C showed that the process reached steady state after 100 min of run and an increase in the molar yield of SO_2 and CO_2 (Fig. 11).

The effects of GHSV on product selectivity of DMS oxidation are illustrated in Fig. 12. The conversion of DMS at all gas hourly space velocities with an O_3-to-DMS mole ratio of 1.8 was 100%. However, selectivity of the partial oxidation products increased as the GHSV increased from 18,785 to 75,000 h^{-1}. The increase can be attributed to a decrease in contact time between reactant and the catalyst with an increasing GHSV. These trends are expected because longer reaction times typically result in deeper oxidation. Fig. 12 illustrates the effects of GHSV on the selectivity of partial oxidation products of DMS oxidation. As the space velocities

Fig. 10. Stability of 10 wt.% V_2O_5/TiO_2 catalyst for product selectivity of the oxidation of DMS with O_3 at selected temperatures. Inlet DMS concentration: 500 ppm; total flow rate: 1000 ml/min; O_3-to-DMS ratio: 1.8; catalyst weight: 2 g.
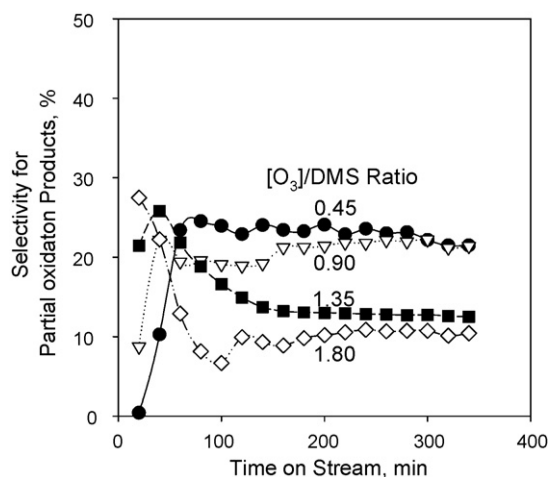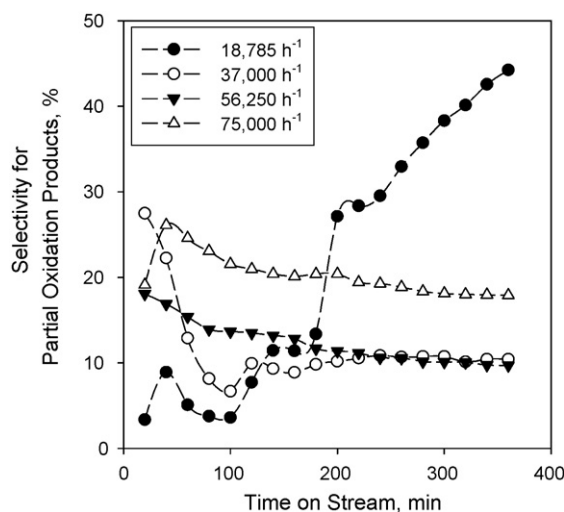

Fig. 12. Stability of 10 wt.% V_2O_5/TiO_2 catalyst for product selectivity of the oxidation of DMS with O_3 at different space velocities. Inlet DMS concentration: 500 ppm; total flow rate: 1000 ml/min; catalyst weight: 2 g, reaction temperature: 200 °C, O_3-to-DMS ratio: 1.8.
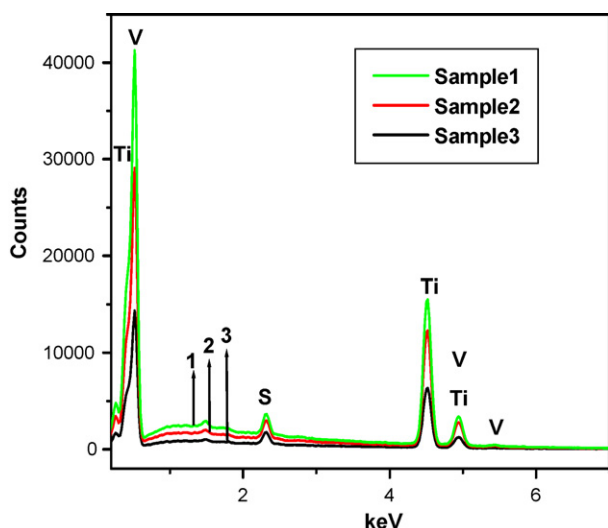
Fig. 13. SEM/EDX analysis for the estimation of sulfur content deposited on the catalysts during the oxidation of DMS with 10% V_2O_5/TiO_2 catalysts. Sample 1: oxidation with O_3 at GHSV, 18,785 h^{-1}; sample 2: with O_3 at GHSV, 75,000 h^{-1}; sample 3: with oxygen at GHSV, 37,000 h^{-1}.

increase, the selectivity to partial oxidation products with O_3 over V_2O_5/TiO_2 (shown in Fig. 12) approached that of gas phase oxidation at the same temperature (shown in Fig. 5).
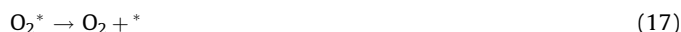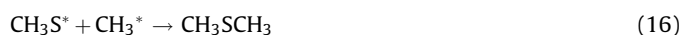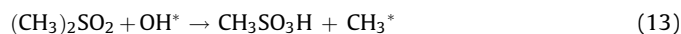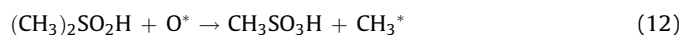
It can also be seen from Fig. 12 that the selectivity of partial oxidation products increased with extended reaction time and a GHSV of 18,500 h^{-1}. This means that the selectivity for complete oxidation products decreased with time-on-stream at lower contact time. The existence of this plateau in product selectivity indicates that a fraction of the active sites are deactivated and unable to convert the ozone. A similar, rapid decline of the performance of Pt/Al_2O_3 catalyst was observed due to the oxidation of DMS, forming irreversible sulfur-poisoning sites [16]. The effect of possible sulfur poisoning on the catalysts during DMS oxidation was studied by determining sulfur deposition on the catalysts using SEM/EDX analyses. The results of the SEM/EDX analyses performed on the catalysts used for DMS oxidation in presence of O_3 at GHSVs of 18,785 and 75,000 h^{-1} and in presence of oxygen at a GHSV of 18,500 h^{-1} are shown in Fig. 13. The catalyst used for DMS oxidation at a GHSV of 18,500 h^{-1} shows a high amount of sulfur deposition (3.97 wt.% of sulfur) when compared to the catalyst used for DMS oxidation at a GHSV of 75,000 h^{-1} (2.33 wt.% of sulfur). These results correspond to the observed product distribution. This suggests that the sulfur deposition on the catalyst is high at low contact time, causing the catalyst deactivation with time during the oxidation of DMS at a GHSV of 18,785 h^{-1}. On the other hand, the catalyst used for the oxidation of DMS with oxygen had lower sulfur content (1.26 wt.% of sulfur) than the catalysts used for the oxidation with ozone, possibly due to the low conversion of DMS ($\approx$20%). Detail analysis and investigation of this effect is need to confirm this observation.

4. Remarks about the reaction pathway

During the oxidation of DMS, carbon dioxide and sulfur dioxide were detected as gas phase reaction products, including dimethyl sulfoxide ($CH_3S(O)CH_3$, DMSO), dimethyl sulfone ($CH_3S(O)_2CH_3$, $DMSO_2$), and while solid–liquid extraction revealed methanesulfenic acid (CH_3SOH, MSEA), and sulfate as reaction products adsorbed on the exposed catalyst. Consequently, based on reaction products and literature data [30,31] the catalytic ozone reaction pathways for DMS degradation and mineralization were proposed.

Detailed gas phase and heterogeneous oxidation of DMS under different condition are reported else where [31,32].

Ozone acts primarily as an electrophile, reacting at points of high electron density in organic substrates. Its reactivity is enhanced by the presence of electron-donating groups and suppressed by the effect of electron-withdrawing substituents. In general, ozone does not completely oxidize organic compounds (in absence of a catalyst) to CO_2 and H_2O. This is because low-molecular-weight partial oxidation products such as acetic acid and oxalic acid are relatively unreactive [18]. Moreover, in the gas phase, the observed reactions are likely due to the radical chain reactions initiated by the decomposition of ozone to O_2 and O. However, when the concentration of the organic compounds is low, the chains do not propagate. The use of a catalyst offers an alternative pathway—the possibility of producing active-surface oxygen species from ozone that can interact with the organic compounds at low temperatures. Decomposition of ozone on the catalyst generated a surface concentration of major reactive active species such as peroxo (O_2^{2-}) groups [18]. The O-initiated oxidation decomposed DMS and produced intermediate species such as (CH_3SCH_2OO-), and then further converted them to stable products [33,34]. The main presumed reactions that included decay reactions of the radicals and the competitive reactions for decomposing sulfur compounds are shown below:

$$O_3 + 2^* \rightarrow O_2^* + O^* \tag{3}$$

$$(CH_3)_2S + O^* \rightarrow (CH_3)_2SO \tag{4}$$

$$(CH_3)_2SO + O^* \rightarrow (CH_3)_2SO_2 \tag{5}$$

$$(CH_3)_2S + {}^* \rightarrow CH_3S^* + CH_3^* \tag{6}$$

$$(CH_3)_2S + O^* \rightarrow CH_3SO + CH_3^* \tag{7}$$

$$CH_3^* + O_2^* \rightarrow CH_2O + OH^* \tag{8}$$

$$CH_2O + O^* \rightarrow CH_2OO \tag{9}$$

$$CH_2OO + O^* \rightarrow CO_2 + H_2O \tag{10}$$

$$(CH_3)_2SO + OH^* \rightarrow (CH_3)_2SO_2H \tag{11}$$

$$(CH_3)_2SO_2H + O^* \rightarrow CH_3SO_3H + CH_3^* \tag{12}$$

$$(CH_3)_2SO_2 + OH^* \rightarrow CH_3SO_3H + CH_3^* \tag{13}$$

$$CH_3SO + O^* \rightarrow SO_2 + CH_3^* \tag{14}$$

$$CH_3S^* + CH_3S^* \rightarrow CH_3^*SSCH_3 \tag{15}$$

$$CH_3S^* + CH_3^* \rightarrow CH_3SCH_3 \tag{16}$$

$$O_2^* \rightarrow O_2 + {}^* \tag{17}$$

In these equations, the asterisk represents surface sites. The decomposition of ozone is closely associated with the oxidation of DMS because both occur simultaneously on the surface.

The main decomposition products of DMS under the different oxidation conditions were used to propose a possible reaction pathway. An analysis of the product confirmed an agreement with known information about the critical steps of ozone oxidation and the radical chemistry of organosulfur compounds. The potential reaction pathway of the oxidation of DMS based on the product distribution is shown in Fig. 14.

The major products observed in GC–MS spectra were DMDS, DMSO, $DMSO_2$, CO_2 and SO_2; methanol, formaldehyde (HCHO), methanethiol (MT), and methyl methanesulfonate (MMS) were observed in trace quantities. The reaction is expected to go through methylsulfonic acid before complete mineralization is achieved.
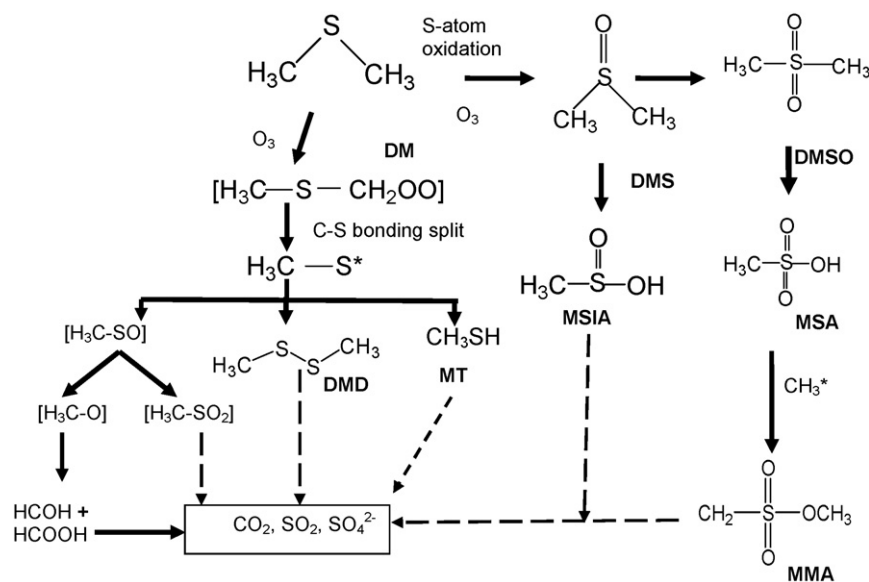
Fig. 14. Plausible scheme of the reaction mechanism for the catalytic oxidation of DMS with ozone. Dashed pathways indicate multiple reaction steps that were skipped before getting to the final product. Samples 1 and 2 correspond to reactions with O_3 at GHSVs of 18,875 and 75,000 h^{-1} and sample 3 is reaction with O_2 at 75,000 h^{-1}. *DMS = dimethyl sulfide; DMDS = dimethyl disulfide; MT = methanethiol; DMSO = dimethyl sulfoxide; $DMSO_2$ = dimethyl sulfone; MSIA = methanesulfinic acid; MSA = methanesulfonic acid; MMA = methane methylsulfonate; HCHO = formaldehyde; HCOOH = formic acid.

This is made evident by the presence of methyl methanesulfonate in the product stream. The initial reaction of DMS with ozone forms the DMSO, which on further oxidation generates $DMSO_2$. The $DMSO_2$ formed will be oxidized further to methanesulfonic acid. These intermediates appeared during almost all the experimental conditions tested, although the latter chemical was not detected. It has been reported in oxygen-based oxidation operations [34].

Methanesulfonic acid formation can be understood through C–S bond cleavage or DMSO oxidation and release of methyl radical. The mechanism of DMS oxidation in the atmosphere and product formation is reported extensively in literature [31–37]. DMS reacts with OH, NO_3, Cl, and halogen oxide radicals in the atmosphere, providing SO_2, DMSO, $DMSO_2$, methanesulfinic acid (MSIA), and methanesulfonic acid (MSA) [34]. MSA on C–S bond cleavage and further oxidation produces SO_2 and CO_2. The oxidation of DMS with ozone may also result in the formation of several intermediates such as [CH_3SCH_2OO], [CH_3S], [CH_3SO], and [CH_3SO_2] and further oxidation with ozone produces SO_2 and CO_2 [31–37].

5. Conclusions

Product studies performed in a flow reactor packed with 10% V_2O_5/TiO_2 catalyst indicated that combined use of ozone and catalyst was essential for low temperature complete destruction of odorous compounds such as DMS. The molar yield of CO_2 and SO_2 was 80–90% and the major partial oxidation product was $DMSO_2$. These results are considerably different than those obtained in studies where oxygen was used for catalytic oxidation of DMS [7,10]. Unlike catalytic incineration of DMS that results in significant deactivation of the catalysts at inlet concentrations less than 100 ppmv, no measurable deactivation was observed [16]. Reaction with oxygen only showed very low conversion of DMS at low temperatures and produced high concentrations of DMSO; high conversions were achieved only at high temperatures (>250 °C). Either the increase in temperature or increase in ozone concentration favors the deep oxidation of DMS to CO_2 and SO_2. Conversions of DMS were high over a wide range GHSVs however mineralization of DMS is reduced at lower GHSV indicating that the

reaction may be mass transfer controlled at lower flow rates. The results of this study agree well with literature values where catalytic (fly ash) ozonation of DMS at room temperature (85 ppmv) resulted in complete conversion of DMS to SO_2 with small quantities of DMSO and $DMSO_2$ extracted from the fly ash [22,23]. In conclusion, ozone-enhanced catalytic oxidation of DMS is a promising low temperature, energy-efficient method for the treatment of total reduced sulfur compounds. A reaction mechanism has been suggested based on both intermediates found in this study and previous mechanisms reported by others for S-containing compounds. However, many fundamental questions remain unanswered. Industrial emissions from Kraft pulping processes consist of many organic and sulfur-containing compound, and moisture. The long-term performance of the catalyst has to be tested under industrial conditions. Research has continued to determine long-term performance of a catalytic ozonation process using a pilot scale system with a feed stream composition similar to a blow tank vent.

References

[1] U.S. EPA, Toxic Release Inventory (TRI) Program, 2005, http://www.epa.gov/tri.
[2] United States Environmental Protection Agency. Fact Sheet: EPA's Final Pulp, Paper, and Paperboard "Cluster Rule"—Overview, EPA-821-F-97-010, 1997.
[3] World Bank Group, Pollution Prevention and Abatement: Pulp and Paper Mills. Technical Background Document, Environment Department, Washington, D.C., 1998.
[4] A.M. Springer, Industrial Environmental Control: Pulp and Paper Industry, third ed., TAPPI Press, Atlanta, GA, 2000, pp. 497–498.
[5] J.E. Yocom, R.A. Duffee, Control. Ind. Odors Chem. Eng. (1970).
[6] R.A. Ross, S.P. Sood, Ind. Eng. Chem. Prod. Res. Dev. 16 (1977) 147–150.

[7] H. Chu, K. Horng, Sci. Total Environ. 209 (1998) 149–156.
[8] H. Ikeda, H. Asaba, Y. Takeuchi, J. Chem. Eng. Jpn. 21 (1988) 91–97.
[9] A. Turk, E. Sakalis, J. Lessuck, H. Karamitsos, O. Rago, Environ. Sci. Technol. 23 (1989) 1242–1245.
[10] H. Chu, W.T. Lee, Sci. Total Environ. 209 (1998) 217–224.
[11] S.W. Benson, Chem. Rev. 78 (1978) 23–35.
[12] J.R. Kastner, K.C. Das, N.D. Melear, J. Hazard. Mater. 95 (2002) 81–90.
[13] C.-H. Wang, H.-S. Weng, Ind. Eng. Res. 36 (1997) 2537–2542.
[14] C.-H. Wang, C.-N. Lee, H.-S. Weng, Ind. Eng. Res. 37 (1998) 1774–1780.
[15] C.-H. Wang, S.-S. Lin, S.-B. Liou, H.-S. Weng, Chemosphere 49 (2002) 389–394.
[16] H. Chu, G.H. Hao, T.K. Tseng, J. Hazard. Mater. B 100 (2003) 301–316.
[17] P. Hunter, S.T. Oyama, Control of Volatile Organic Compound Emissions: Conventional and Emerging Technologies, John Wiley & Sons, New York, 2000.
[18] S.T. Oyama, Catal. Rev. Sci. Eng. 42 (2000) 279–322.
[19] F.J. Beltran, F.J. Rivas, L.A. Fernandez, P.M. Alvarez, R. Montero-de-Espinosa, Ind. Eng. Chem. Res. 41 (2002) 6510–6517.
[20] D.S. Pines, D.A. Reckhow, Environ. Sci. Technol. 36 (2002) 4046–4051.
[21] U. Jans, J. Hoigne, Ozone Sci. Eng. 20 (1998) 67–90.
[22] J.R. Kastner, Q. Buquoi, R. Ganagavaram, K.C. Das, Environ. Sci. Technol. 39 (2005) 1835–1842.
[23] J.R. Kastner, Q. Buquoi, K.C. Das, N.D. Melear, Environ. Sci. Technol. 37 (2003) 2568–2574.
[24] G. Busca, P. Tettarelli, E. Tronconi, P. Forzatti, J. Solid State Chem. 67 (1987) 91–97.
[25] G. Busca, A.S. Elmi, N. Forzatti, J. Phys. Chem. 91 (1987) 5263–5269.
[26] E. Tronconi, A.S. Elmi, N. Ferlazzo, P. Forzatti, G. Busch, P. Tittarelli, Ind. Eng. Chem. Res. 26 (1987) 1269–1275.
[27] G. Gordon, W.J. Cooper, R.G. Rice, G.E. Pacey, Disinfectant Residual Measurement Methods, second Edition, AWWARF and AWWA, Denver, CO, 1992.
[28] C.B. Almquist, E. Sahle-Demessie, S. Chandra Sehjer, J. Sowash, Environ. Sci. Technol. 41 (2007) 475–4760.
[29] G.G. Vining, Statistical Methods for Engineers, Duxbury-Brooks/Cole, Pacific Grove, CA, 1998.
[30] K. Demeestere, J. Dewulf, B. De Witte, H.V. Langehhove, Appl. Catal. B: Environ. 60 (2005) 93–106.
[31] D.D. Lucas, R.G. Prinn, Atmos. Chem. Phys. 5 (2005) 1505–1525.
[32] C.H. Tsai, Y.J. Haung, J.C. Chen, W.T. Liao, G.C. Fang, J. Air Waste Mange. Assoc. 53 (2003) 1225–1232.
[33] W.S. Nip, D.L. Singleton, R.J. Cvetanovic, J. Am. Chem. Soc. 103 (1981) 3526–3530.
[34] A.V. Vorontsov, E.V. Savinov, L. Davydov, P.G. Smirniotis, Appl. Catal. B 32 (2001) 11–24.
[35] C. Wilson, D.M. Hirst, Prog. React. Kinet. 21 (1996) 69–132.
[36] H. Sievering, J. Boatman, E. Gorman, Y. Kim, L. Anderson, G. Ennis, M. Luria, S. Pandis, Nature 360 (1992) 571–573.
[37] I. Barnes, J. Hjorth, N. Mihalopoulos, Chem. Rev. 106 (2006) 940–975.